Wind field determination from multiple Spinner-Lidar line-of-sight measurements using linearized CFD

Astrup, Poul; Mikkelsen, Torben Krogh; van Dooren, Marijn Floris

Link to article, DOI:
10.11581/dtu:00000053

Publication date:
2017

Document Version
Publisher's PDF, also known as Version of record

Wind field determination from multiple Spinner-Lidar line-of-sight measurements using linearized CFD

Poul Astrup, Torben Mikkelsen, Marijn Floris van Dooren

DTU Wind Energy E-0102

February 2017

ISBN: 978-87-93278-57-8

DTU Wind Energy
Department of Wind Energy

Authors: Poul Astrup, Torben Mikkelsen, Marijn Floris van Dooren

Title: Wind field determination from multiple Spinner-Lidar line-of-sight measurements using linearized CFD

Summary (max 2000 characters):

In order to determine the flow field in front of or behind a wind turbine from measurements with a spinner or nacelle mounted lidar, the “LINCOM method”, i.e. linearized flow equations solved in Fourier space, is applied to such measurements in an iterative way. The calculation system *z*-axis points horizontally with the wind, i.e. for the inlet flow determination it points from the measurement plane towards the lidar, for a wake flow determination from the lidar to the measurement plane. The *y*-axis points vertically upwards, and the *x*-axis is horizontal, *x,y,z* forming a right handed coordinate system.

Contract no.:

Project no.:
44589 E-3

Sponsorship:

Front page:

Pages: 24
Tables: 0
References: 2

Technical University of Denmark
Department of Wind Energy
Frederiksborgvej 399
DK-4000 Roskilde
Denmark

Telephone : ?????

www.vindenergi.dtu.dk

Content

Summary

In order to determine the flow field in front of or behind a wind turbine from measurements with a spinner or nacelle mounted lidar, the “LINCOM method”, i.e. linearized flow equations solved in Fourier space, is applied to such measurements in an iterative way. The calculation system *z*-axis points horizontally with the wind, i.e. for the inlet flow determination it points from the measurement plane towards the lidar, for a wake flow determination from the lidar to the measurement plane. The *y*-axis points vertically upwards, and the *x*-axis is horizontal, *x,y,z* forming a right handed coordinate system.

1. Introduction

The “LINCOM method”, Astrup et al. (1992), Troen and de Baas (1986), is applied to spinner lidar measurements in a disk in front of or behind a wind turbine rotor. The *z*-axis points horizontally with the wind, the *y*-axis points vertically upwards, and the *x*-axis is horizontal. *x,y,z* forms a right handed coordinate system.

2. The “LINCOM method”

The “LINCOM method” is based on solving linearized momentum equations plus the mass equation in Fourier space, and the equations are for the spatial wind speed variations, perturbations, around an invariant flow, a plug flow.

With U,V,W being the plug flow and u,v,w the perturbations, i.e. the real wind’s deviation from the plug flow, the mentioned linearized equations read in real space:

$$U\frac{\partial u}{\partial x}+V\frac{\partial u}{\partial y}+W\frac{\partial u}{\partial z} = -\frac{\partial}{\partial x}\frac{p}{\rho}+K_{\mathrm{xy}}\left[\frac{\partial^2 u}{\partial x^2}+\frac{\partial^2 u}{\partial y^2}\right]+K_z\frac{\partial^2 u}{\partial z^2}$$
$$U\frac{\partial v}{\partial x}+V\frac{\partial v}{\partial y}+W\frac{\partial v}{\partial z} = -\frac{\partial}{\partial y}\frac{p}{\rho}+K_{\mathrm{xy}}\left[\frac{\partial^2 v}{\partial x^2}+\frac{\partial^2 v}{\partial y^2}\right]+K_z\frac{\partial^2 v}{\partial z^2}$$
$$U\frac{\partial w}{\partial x}+V\frac{\partial w}{\partial y}+W\frac{\partial w}{\partial z} = -\frac{\partial}{\partial z}\frac{p}{\rho}+K_{\mathrm{xy}}\left[\frac{\partial^2 w}{\partial x^2}+\frac{\partial^2 w}{\partial y^2}\right]+K_z\frac{\partial^2 w}{\partial z^2}$$
$$\frac{\partial u}{\partial x}+\frac{\partial v}{\partial y}+\frac{\partial w}{\partial z} = 0$$

By Fourier transforming in *x*- and *y*-directions, applying wave numbers k and m respectively, the equations become:

$$\left[i\,(\mathrm{kU}+\mathrm{mV})+K_{\mathrm{xy}}(k^2+m^2)\right]u+\mathrm{ikp}+W\frac{\partial u}{\partial z}-K_z\frac{\partial^2 u}{\partial z^2} = 0$$
$$\left[i\,(\mathrm{kU}+\mathrm{mV})+K_{\mathrm{xy}}(k^2+m^2)\right]v+\mathrm{imp}+W\frac{\partial v}{\partial z}-K_z\frac{\partial^2 v}{\partial z^2} = 0$$
$$\left[i\,(\mathrm{kU}+\mathrm{mV})+K_{\mathrm{xy}}(k^2+m^2)\right]w+\frac{\partial p}{\partial z}+W\frac{\partial w}{\partial z}-K_z\frac{\partial^2 w}{\partial z^2} = 0$$
$$\mathrm{iku}+\mathrm{imv}+\frac{\partial w}{\partial z} = 0$$

where now u,v,w,p are the Fourier components for real space variables $u,v,w,p/\rho$.
These equations are solved by selecting a decent solution in the *z*-direction:

$$(u,v,w,p)_z = (u,v,w,p)_0\exp(\alpha\, z)$$

where, in the case of looking into the wind, α needs to be positive for the perturbations to vanish for $z \to -\infty$ and for the case of looking into the wake, α needs to be negative for the perturbations to vanish for $z \to \infty$.

With $C = i(\mathrm{kU} + \mathrm{mV}) + K_{xy}(k^2 + m^2) + W\alpha - K\alpha^2$ the equations can be written in the following matrix form:

$$\begin{bmatrix} C & 0 & 0 & \mathrm{ik} \\ 0 & C & 0 & \mathrm{im} \\ 0 & 0 & C & \alpha \\ \mathrm{ik} & \mathrm{im} & \alpha & 0 \end{bmatrix} \begin{pmatrix} u \\ v \\ w \\ p \end{pmatrix} = \begin{pmatrix} 0 \\ 0 \\ 0 \\ 0 \end{pmatrix}$$

For the determinant $\mathrm{Det} = C^2(k^2 + m^2 - \alpha^2)$ not equal to zero, the only solution is $u,v,w,p = 0$, which is not so interesting. Interesting solutions therefore have to be searched for $Det = 0$, which requires either $C = 0$ or $\alpha^2 = k^2 + m^2$.

Outer solution

The solution based on $\alpha^2 = k^2 + m^2$ is called the outer solution and is inviscid. The outer length scale is defined as $L = 1/|\alpha| = 1/\sqrt{k^2 + m^2}$.

From the third line in the matrix equation it is seen, that $\mathrm{wC} + \alpha p = 0$ and from this and the first two lines:

$p = -\mathrm{Cw}/\alpha = -\mathrm{CLw}$
$u = -\mathrm{ikp}/C = \mathrm{ikLw}$ for the lidar looking into the wind, α positive
$v = -\mathrm{imp}/C = \mathrm{imLw}$

$p = -\mathrm{Cw}/\alpha = \mathrm{CLw}$
$u = -\mathrm{ikp}/C = -\mathrm{ikLw}$ for the lidar looking into the wake, α negative
$v = -\mathrm{imp}/C = -\mathrm{imLw}$

With other words, for the outer solution the variables are coupled and only needs a single boundary equation in one of u,v,w,p to give them all.

Inner solution

$C = 0$ leads to the so called inner solution. Only the mass equation is left:

$$\mathrm{iku} + \mathrm{imv} + \alpha w = 0$$

and α is to be found from

$$C = i(\mathrm{kU} + \mathrm{mV}) + K_{xy}(k^2 + m^2) + W\alpha - K\alpha^2 = 0$$

Boundary conditions for two of the unknown wind speed components are needed for an inner solution.
The equation system is linear, and so the sum of an inner and an outer solution is also a solution.
The real space solution is found from the Fourier space solution by applying a Fast Fourier transform.

3. Application of the outer solution

For the flow through a disk in front of a wind turbine, we look at the outer solution only and so need and can use only one boundary condition. For that we use the *w*-perturbation, iterating on

it until the calculated wind field projected onto the lidar radials give the measured line of sight wind speeds. That this is possible is not quite easy to see, but it is, if there are not too many measurement points and if each has its own grid cell.

Figure 1 shows a symmetric test case with 121 measurement points and 21*21 grid points. Figure 2 to 4 show the calculated wind speeds in the measurement plane, the axial (*w*-), the horizontal transverse (*u*-), and the vertical transverse (*v*-) components. Figure 5 shows the calculated line of sight wind speeds turned into a grid plot, and figure 6 compares the calculated line of sight speeds to the measured, spot on.

4. Handling of skew flows

It turns out, that for a skew flow the above method still finds a solution that matches the lidar line of sight wind speeds, but not a correct one. If the skewness, i.e. the average U- and V-components over the plane, are hard coded, it goes much better. With other words, it is necessary to find a reasonable average U and V before the perturbations can be determined with reasonable accuracy with the above method. This determination is not based on the single scan but on a reasonable high number of scans, i.e. the number of scans within one scanning file, here typically 30 scans.

For each lidar ray the line of sight wind speed due to this average flow is the dot product of the ray unit vector and the searched average wind field:

$$U_{i,\mathrm{los}} = (x,y,z)_i \cdot (U,V,W) = x_i U + y_i V + z_i W \qquad (4.1)$$

Having the y-axis vertical, I.e. perpendicular to the ground, V can be approximated by zero.

Then separate summing over the points for which x is positive and over those for which x is negative gives

$$\sum U_{i,\mathrm{los,x>0}} = U \sum_{x>0} x_i + W \sum_{x>0} z_i \qquad (4.2)$$

$$\sum U_{i,\mathrm{los,x<0}} = U \sum_{x<0} x_i + W \sum_{x<0} z_i \qquad (4.3)$$

With an approximately equal distribution of z for x >0 and x<0 the two W terms are approximately equal, and a reasonable value for U is then obtained as

$$U = \frac{\sum U_{i,\mathrm{los,x>0}} - \sum U_{i,\mathrm{los,x<0}}}{\sum_{x>0} x_i - \sum_{x<0} x_i} \qquad (4.4)$$

5. Real case

A real case lidar setup is shown in figure 5. There nacelle is tilted and the focal length is constant, meaning that the measurements are made on a spherical surface, not on a plane. This is overcome by anticipating the flow to not deform between the calculation plane and the

sphere, or with other words, a measurements at the sphere is anticipated measured at the location in the calculation plane having the same x,y and by a ray with the correct unit vector.

A real case lidar scan plane is shown in figure 8. However, as the “spinner” lidar in this case is positioned on top of the nacelle and not within the spinner, the passing wings invalidate part of the measurements and also close to the ground there are problems. An analysis indicates that the valid measurements are those above 6 m/s, so only these are used here, and this reduces the amount of measurements from 18750 to 8486. With 400 measurements per second the measuring period has been almost 50 seconds, and as many measurement points lay close, figure 9, the measured wind speeds at close points vary pretty much. In this case the method giving the good results above fails.

In order to tackle this case it has been necessary to average near laying measurements and to make sure there is only one per grid cell. The way this has been done is to average around grid points, these getting “measured” speed values formed as a weighted average of the nearby positioned real measurements, figure 10.
When calculating the radial wind speeds in the real measurement points from the found wind field, a four point interpolation between the four grid points surrounding the measurement point is used. The weight a grid point here has on a measurement point is also used for the measurement point’s relative weight on the grid point when finding the “measured” value at that grid point, but only measurements with such a weight above 0.1 is used in this respect. This somewhat arbitrary limit is for avoiding that two measurement points very close to each other can get highly different weights, which is otherwise the case if they are also very but differently close to a neighbour grid point.
This method give exact correspondence between the grid point “measurements” and the final calculated radial wind speed components for the grid points, but not exactly for the real measurement points. Figure, 11, 12 and 13 show the result. Although figure 11 doesn’t look good, it is not at all bad. It is the wide spread of measurements in close laying points that make it look no good. The measurements averaged to the grid points are reproduced exactly.
The close lying measurement points of figure 9 and 10 belong to different scans. If only the first scan is used, figure 14, the resulting picture looks more convincing, figure 15. Some off layers are still present as due to the scan path crossing itself there are also close laying measurement points measured at different time in a single scan. Figure 16, 17, and 18 show the found u, v, and w (axial) wind speed components for the single scan case, and figures 19 and 20 show the interpolated line of sight data, measured and calculated.

6. Conclusion

Applying only the so called outer solution of the “LINCOM method” one boundary condition is sufficient to get the full 3D u,v.w perturbation flow field. Here the w-perturbation is used for this boundary condition. Iterations are performed in the w-perturbation so that the final calculated wind field gives wind speeds along the lidar line of sights, that at most points specified are very close to those measured. Not well predicted measurements are typically pretty much different from other measurements close by.

The “LINCOM method” solves the flow equations for speed component perturbations in Fourier space by adopting exponential decreasing perturbation coefficients for increasing distance from the calculation plane in direction away from the lidar.

There is no indication that the flow field away from the calculation plane can be calculated reasonably using this method.

7. Figures

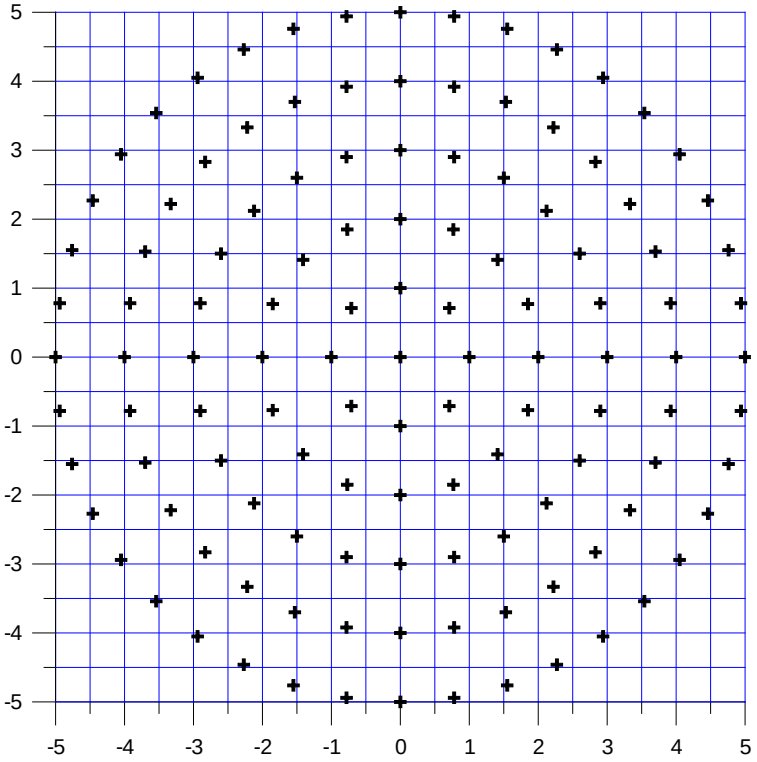

Figure 1: 21*21 calculation grid and 121 artificial lidar measurement points.

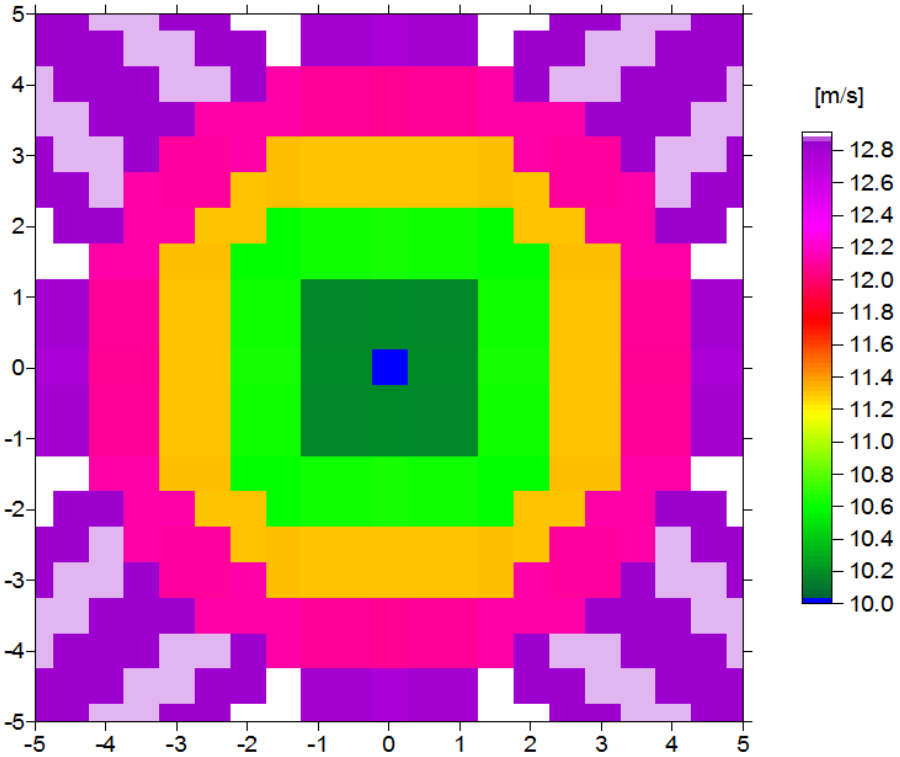

Figure 2: w-component (parallel to scanner lidar center line).

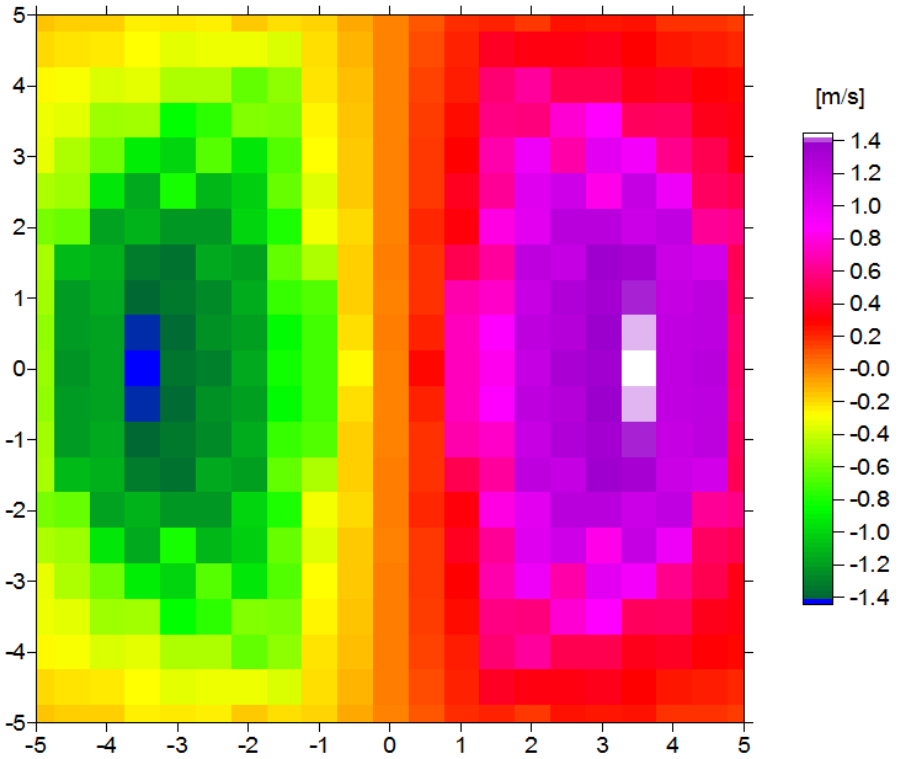

Figure 3: u-component. Output.

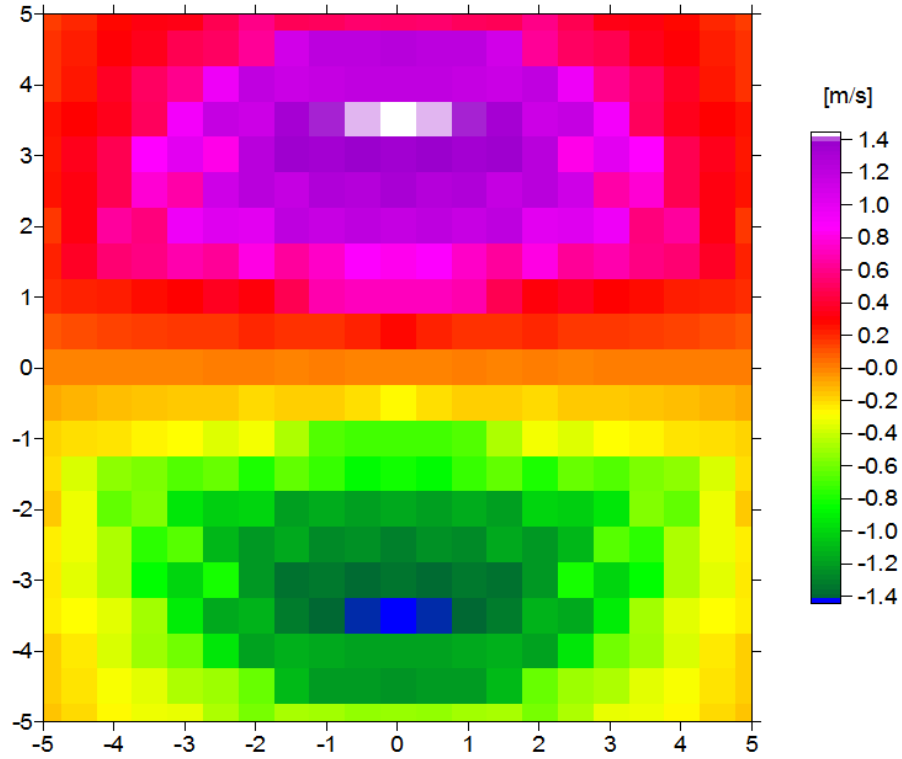

Figure 4: v-component. Output.

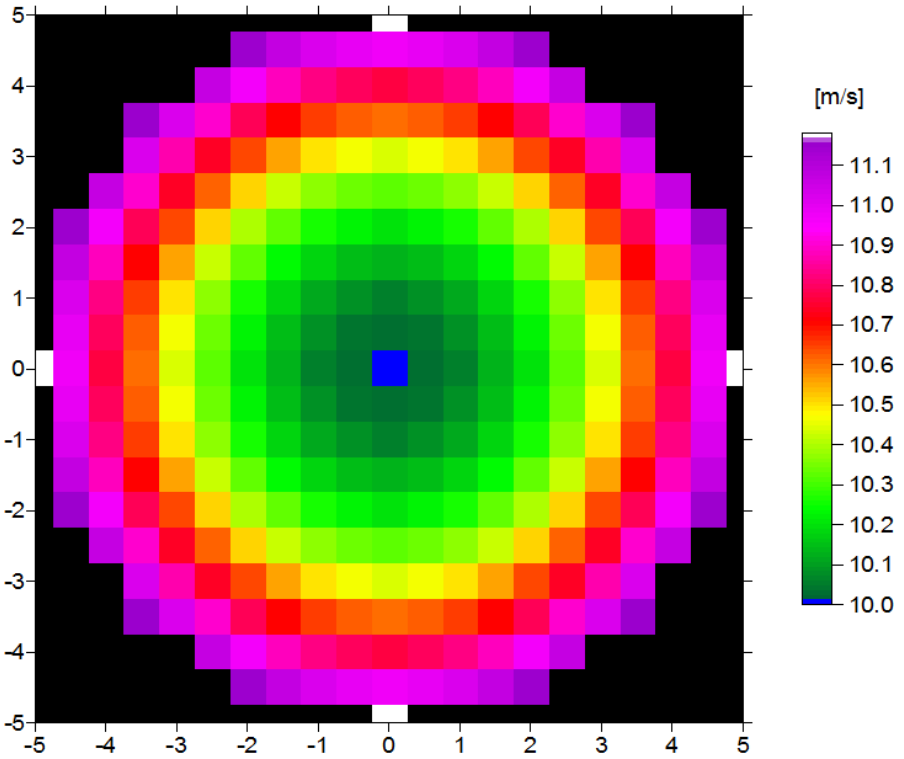

Figure 5: Calculated wind field projected onto lidar measurement directions.

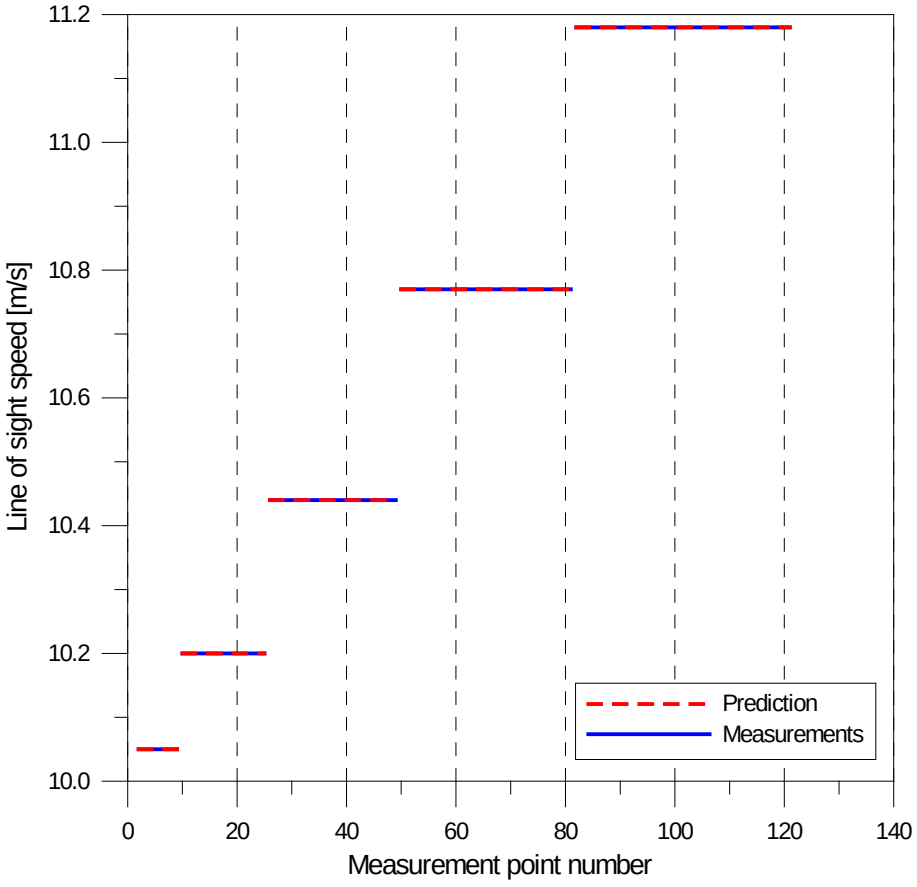

Figure 6: Calculated and measured line of sight wind speeds.

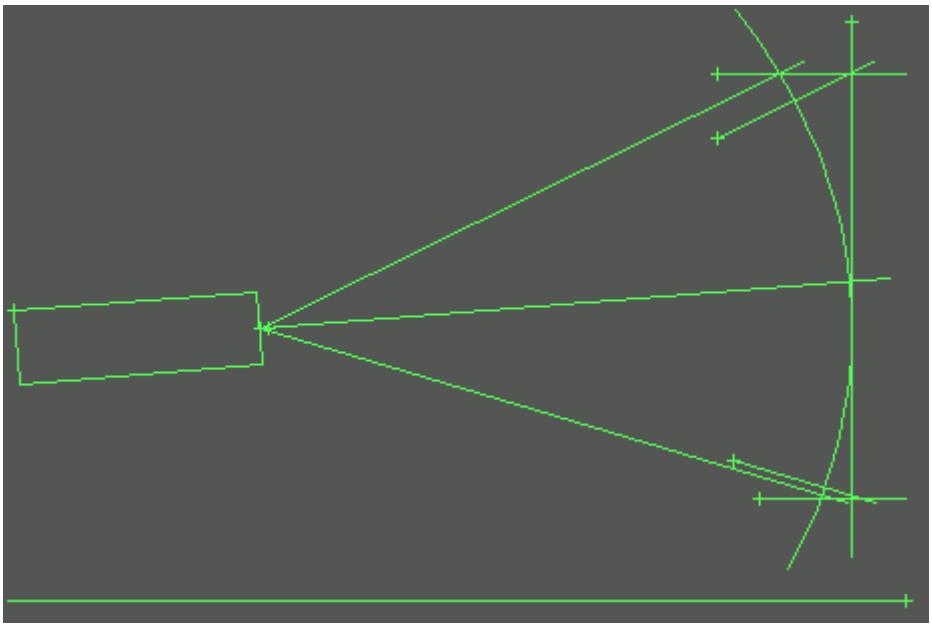

Figure 7: Lidar tilted 5 degree upwards. Measurements made over a spherical surface, i.e. focal length constant over the scan. The calculation area is plane and vertical. The ray measurements are “moved” horizontally from sphere to plane.

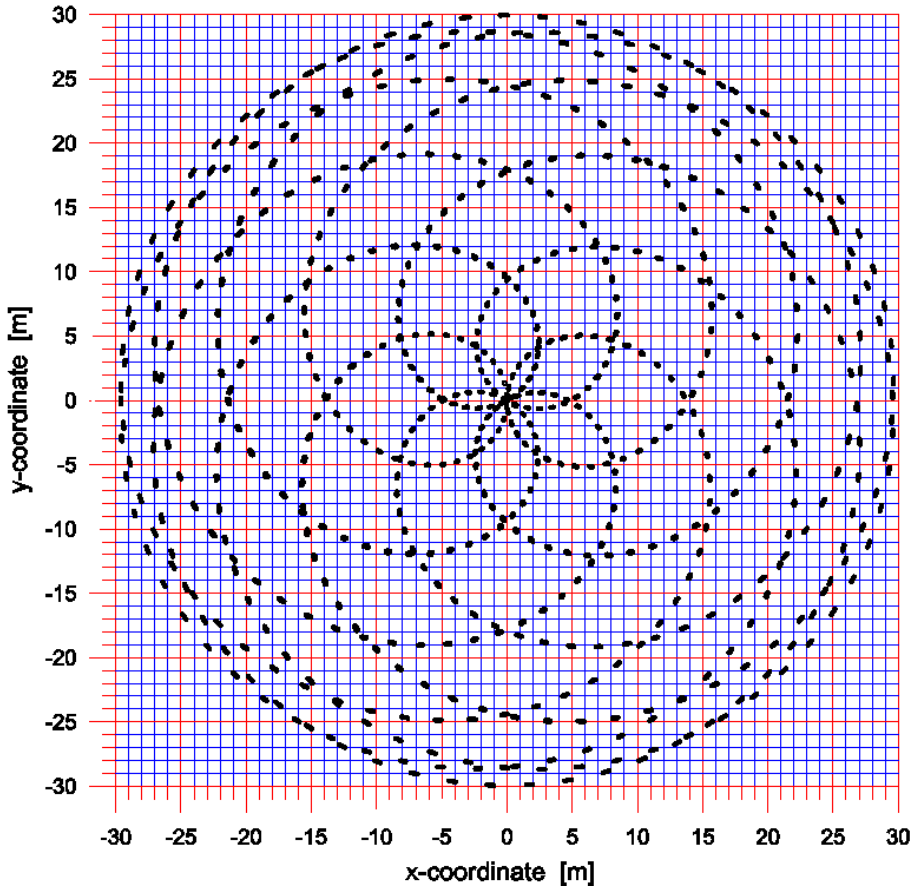

Figure 8. A real lidar scan diagram.

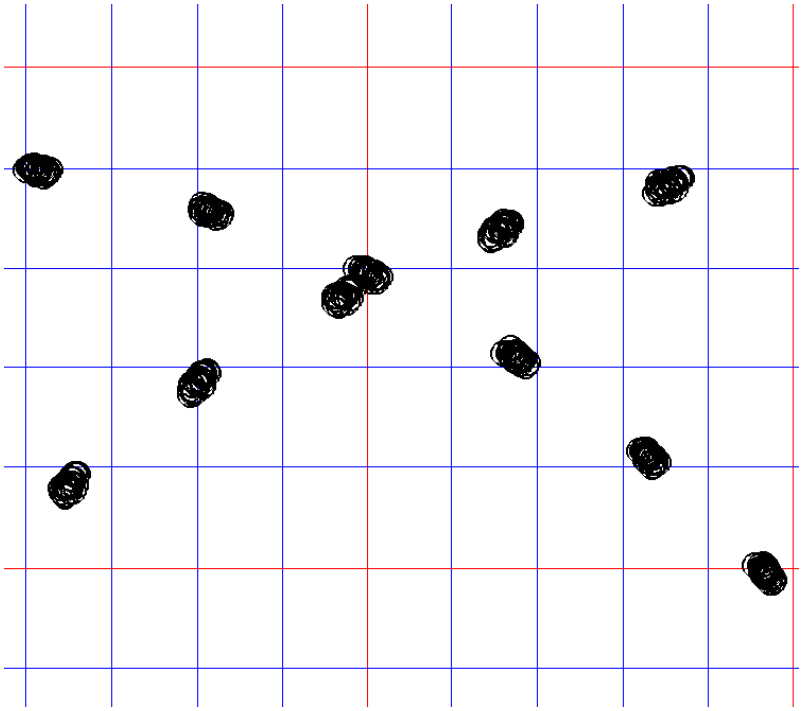

Figure 9: Enlarged cutout of figure 8. Each circle is a measurement point. Close lying measurements are from different scans.

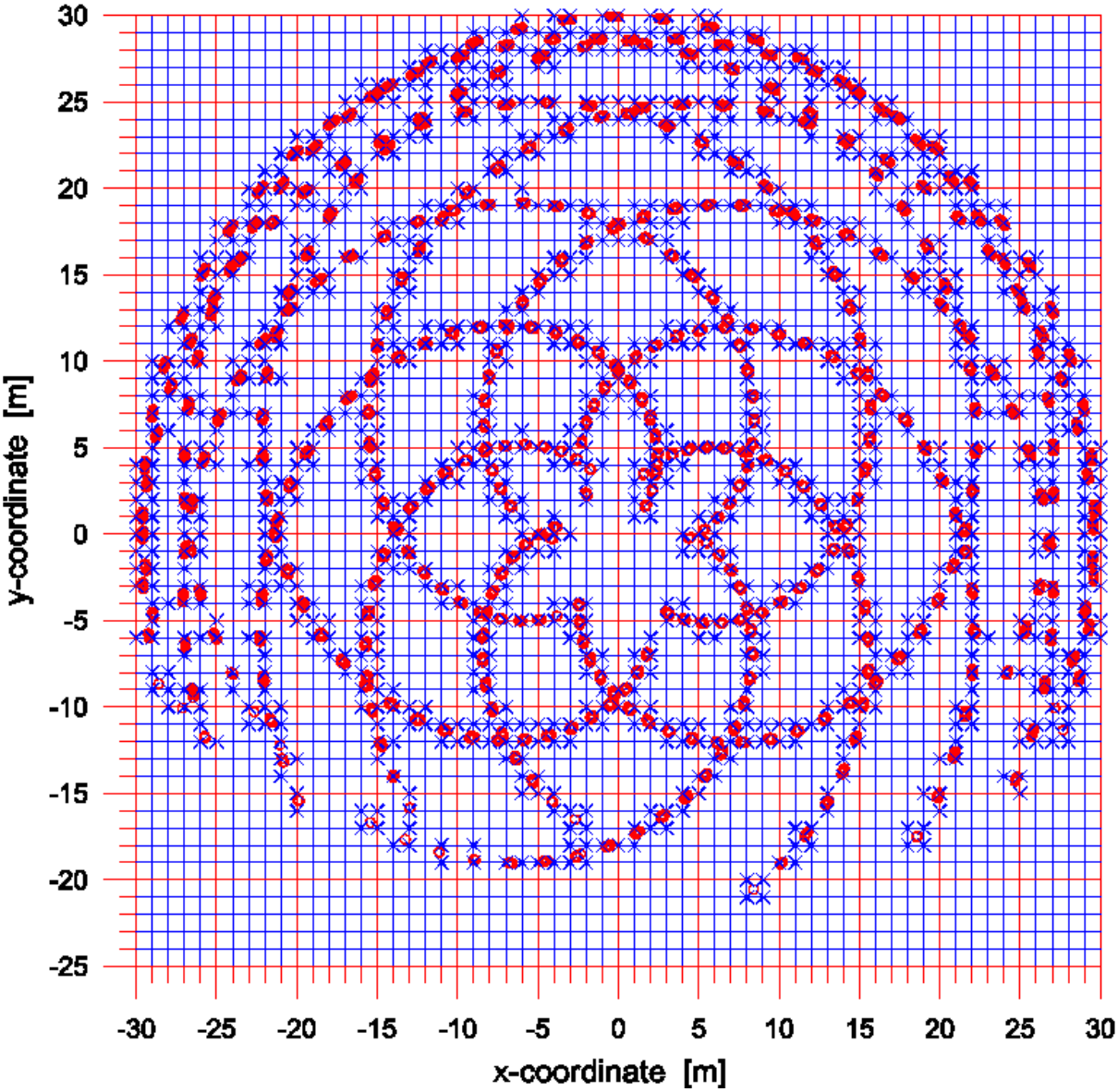

Figure 10: Red circles are the 8486 real measurement points with wind speeds > 6 m/s, the blue X's are the grid points used as "measurement" points for the flow field calculation.

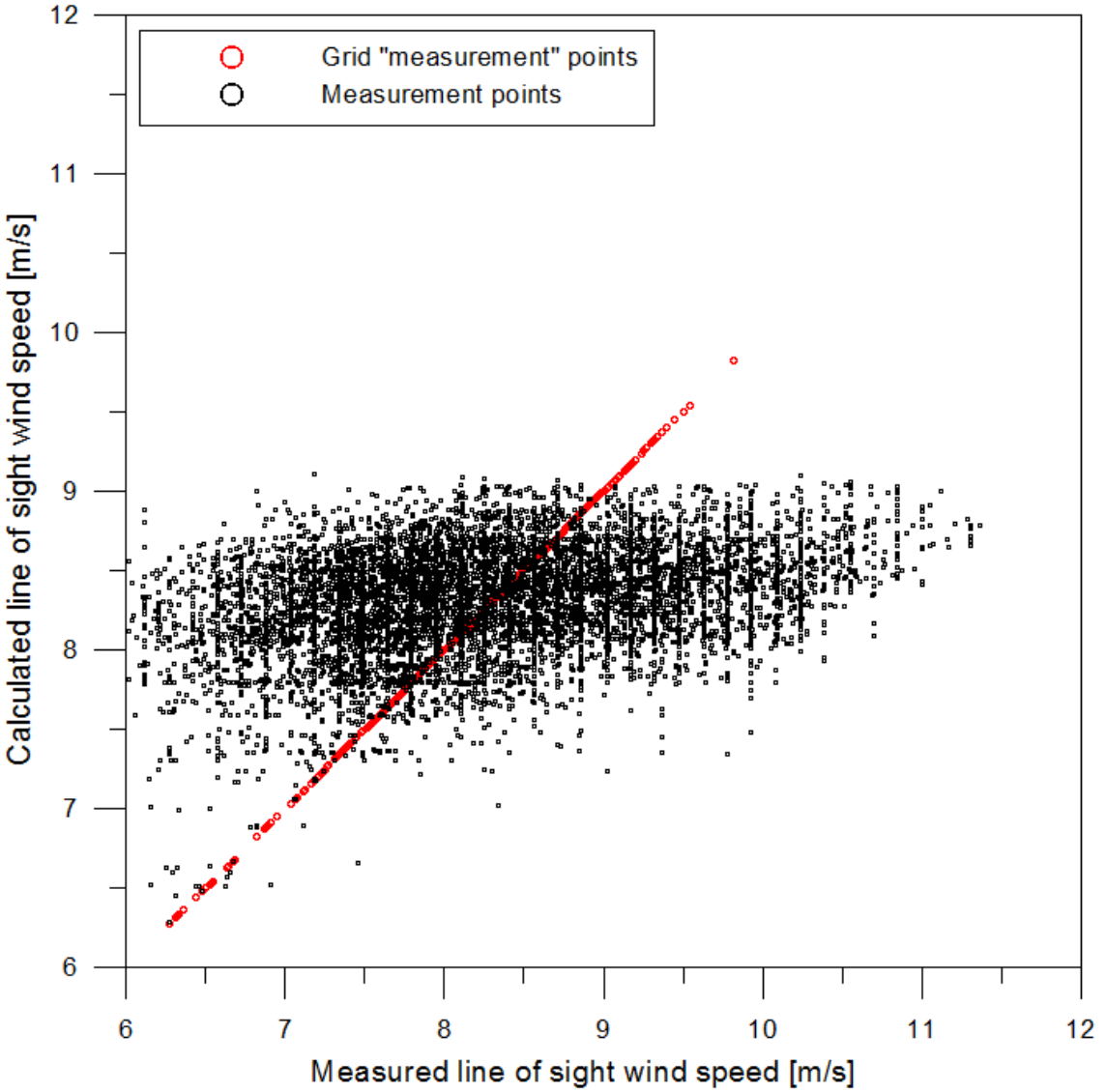

Figure 11: Red circles: The grid “measurements” are met exactly. Black circles: The real measurements are not - due to large spread of measurements in close laying points.

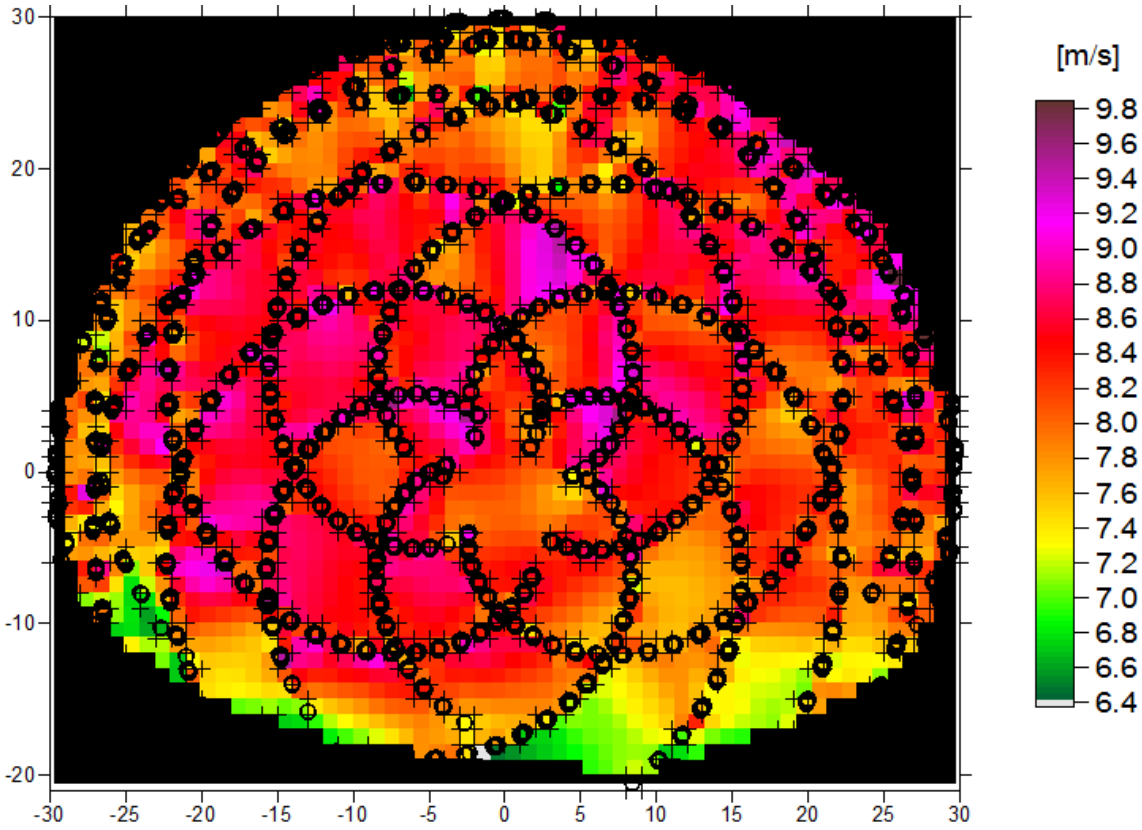

Figure 12: Measured lidar line of sight wind speeds, interpolated to the grid.

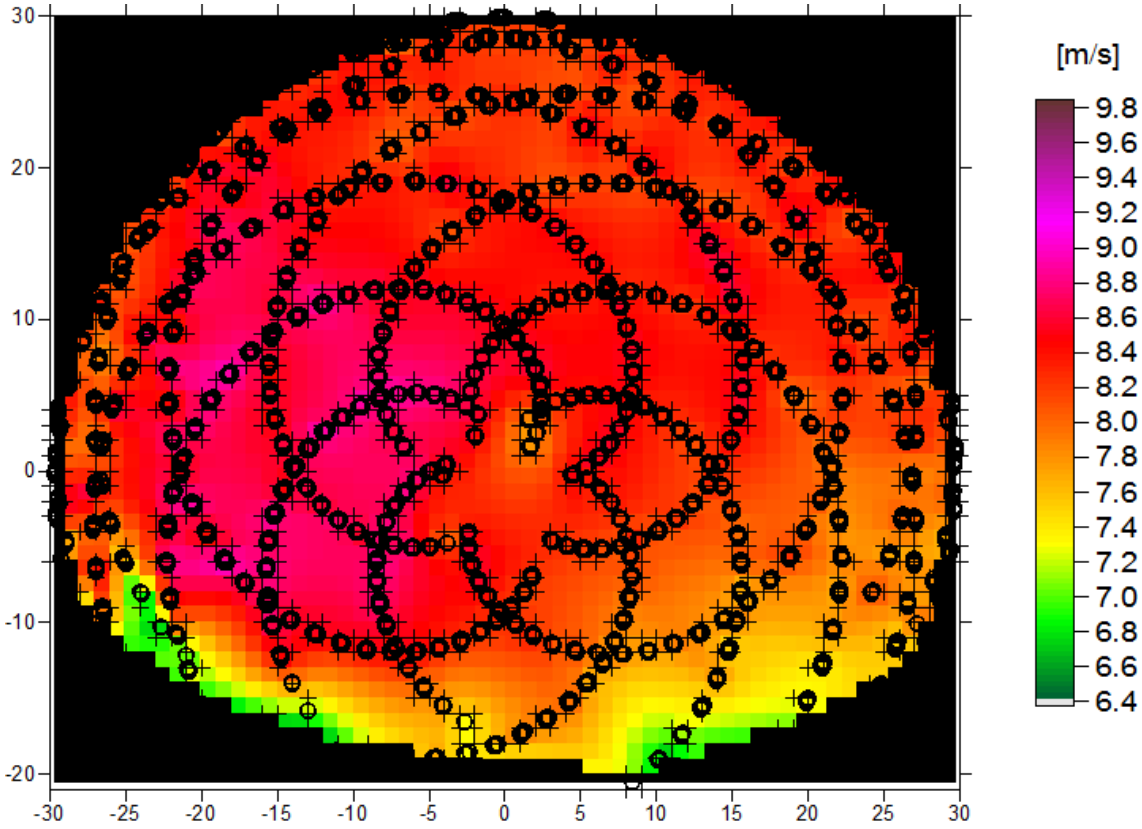

Figure 13: Calculated line of sight wind speeds for the real measurement points, interpolated to the grid.2

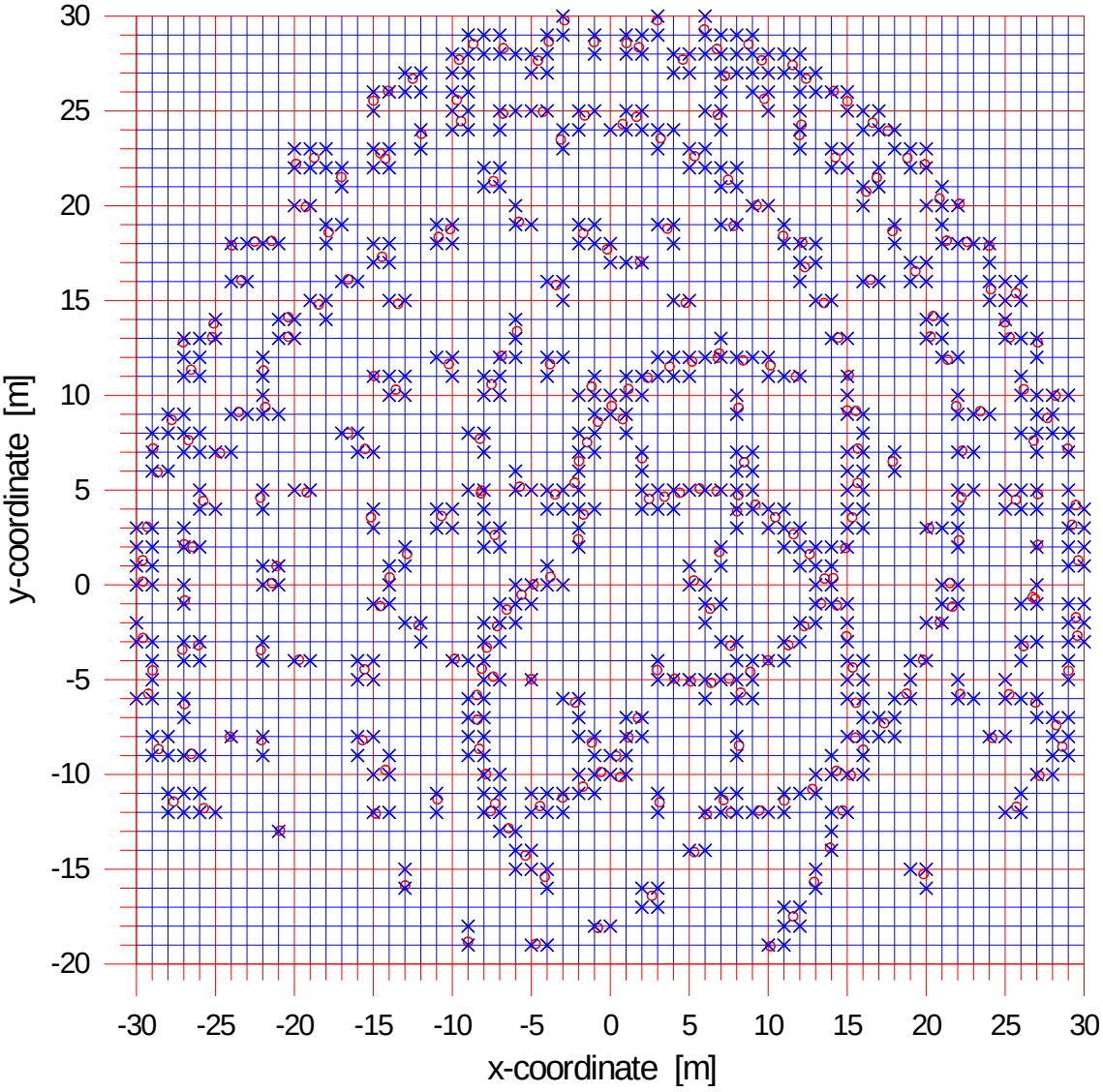

2

Figure 14: Red circles are real measurement points for first scan only and with wind speeds > 6 m/s, i.e. 311 points in this case. The blue X's are the 732 grid points used as grid "measurement" points for the flow field calculation.

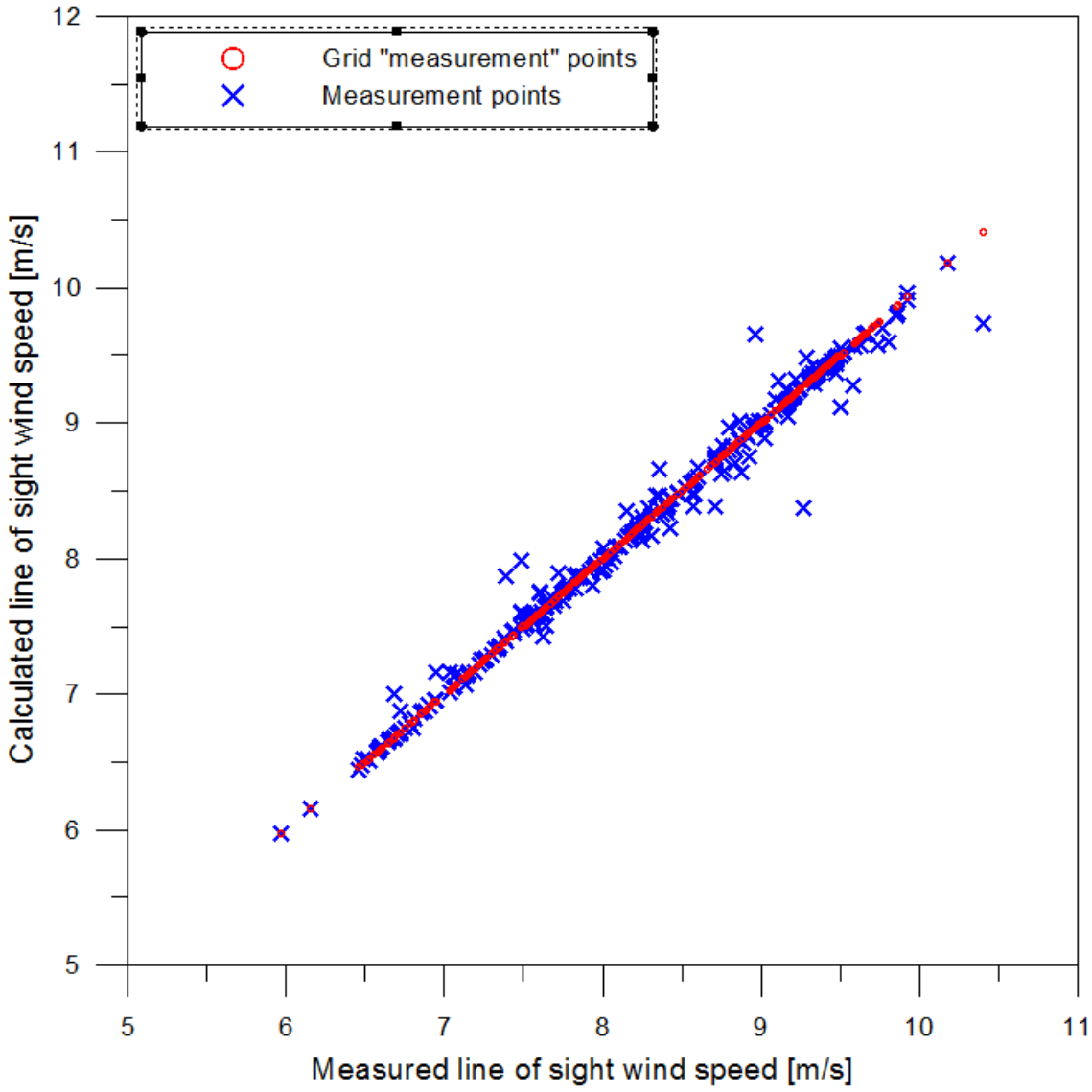

Figure 15. With only 311 measurements, i.e. a single lidar scan.

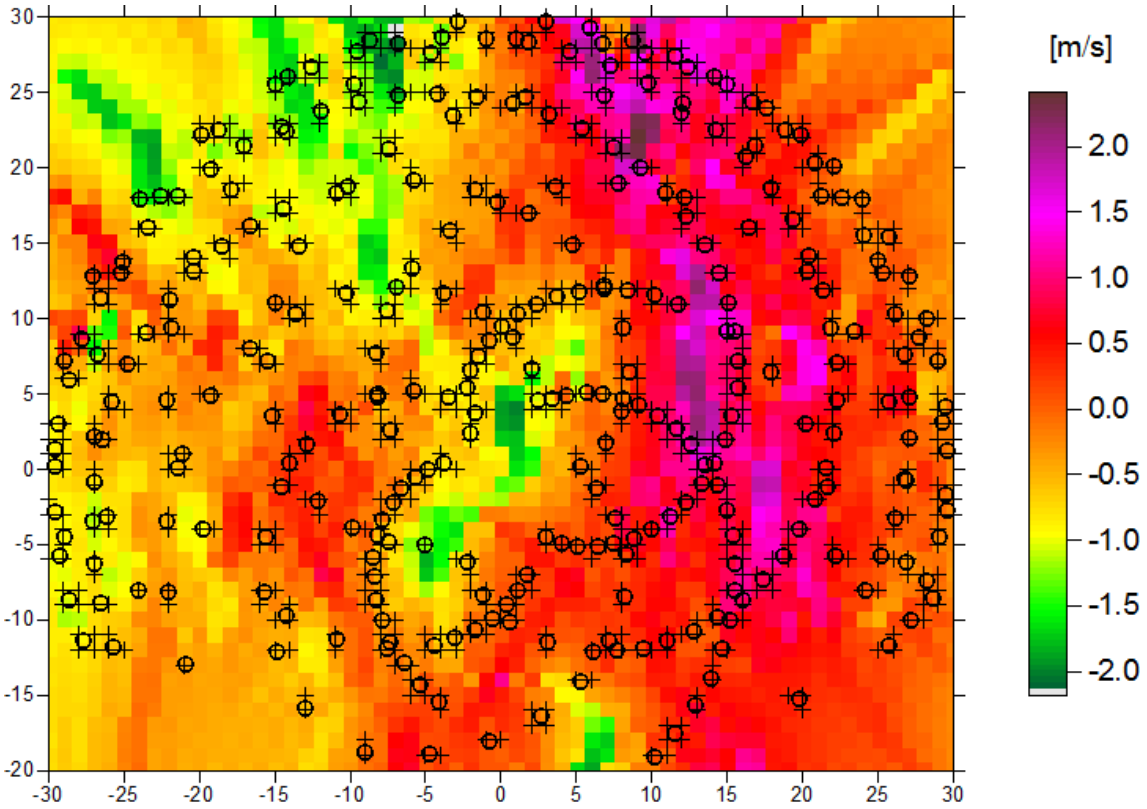

Figure 16. Calculated u-component in the single scan case.

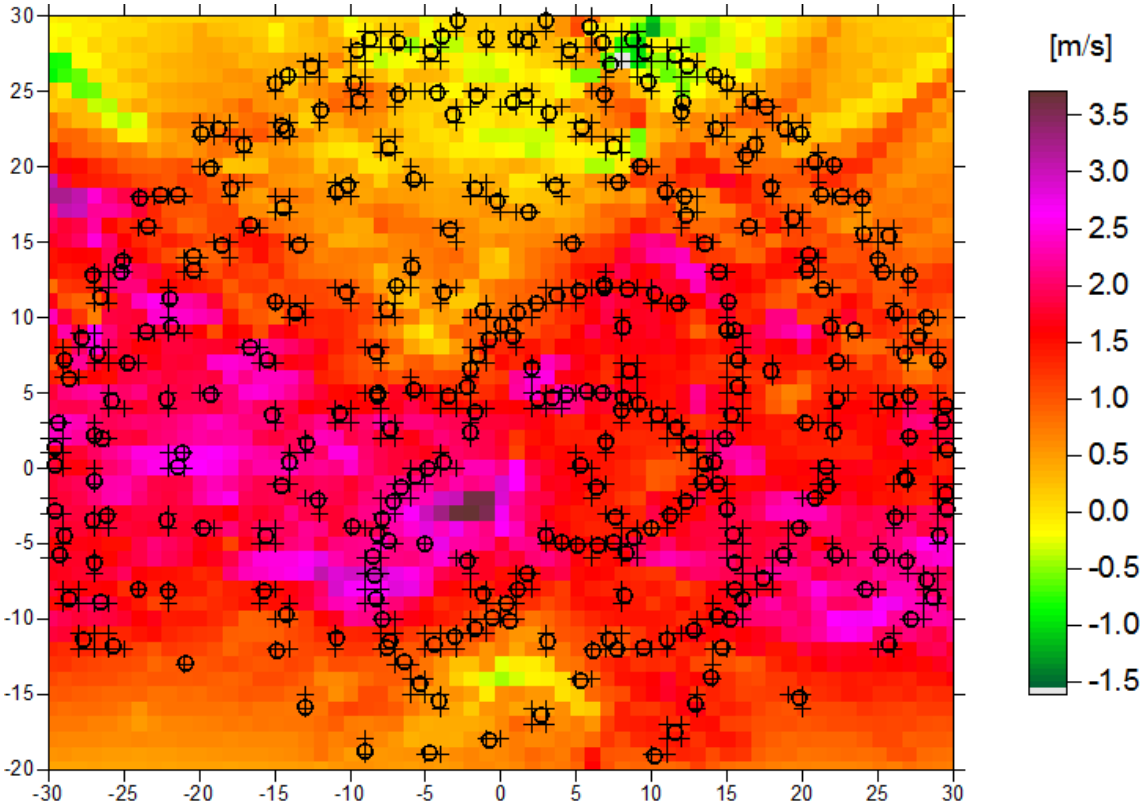

Figure 17. Calculated v-component in the single scan case.

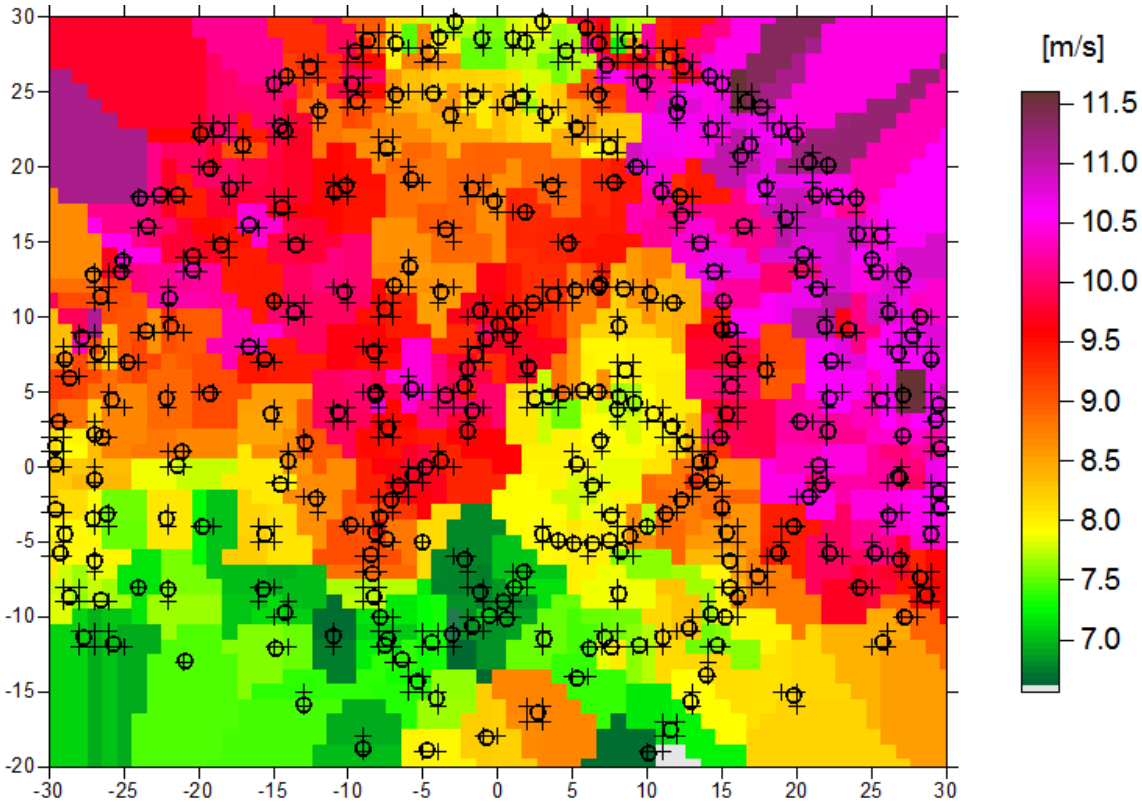

Figure 18. Calculated (axial) w-component in the single scan case.

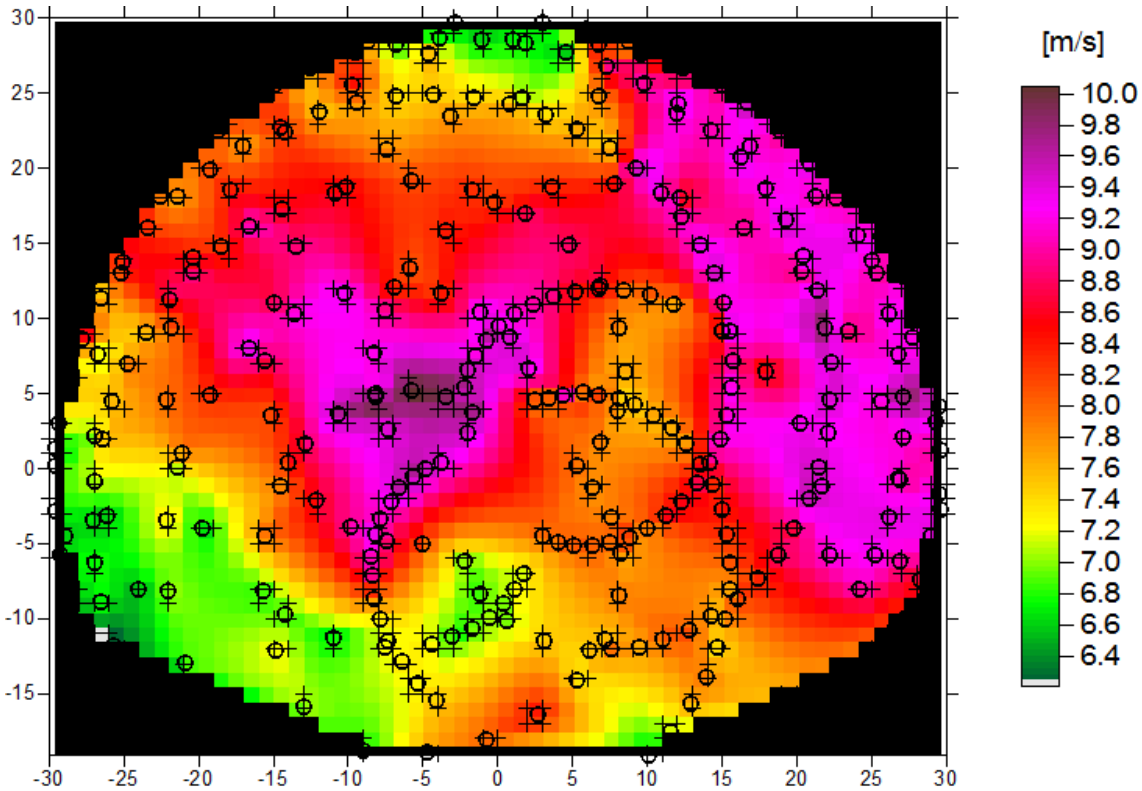

Figure 19: Measured line of sight wind speeds, interpolated to the grid.

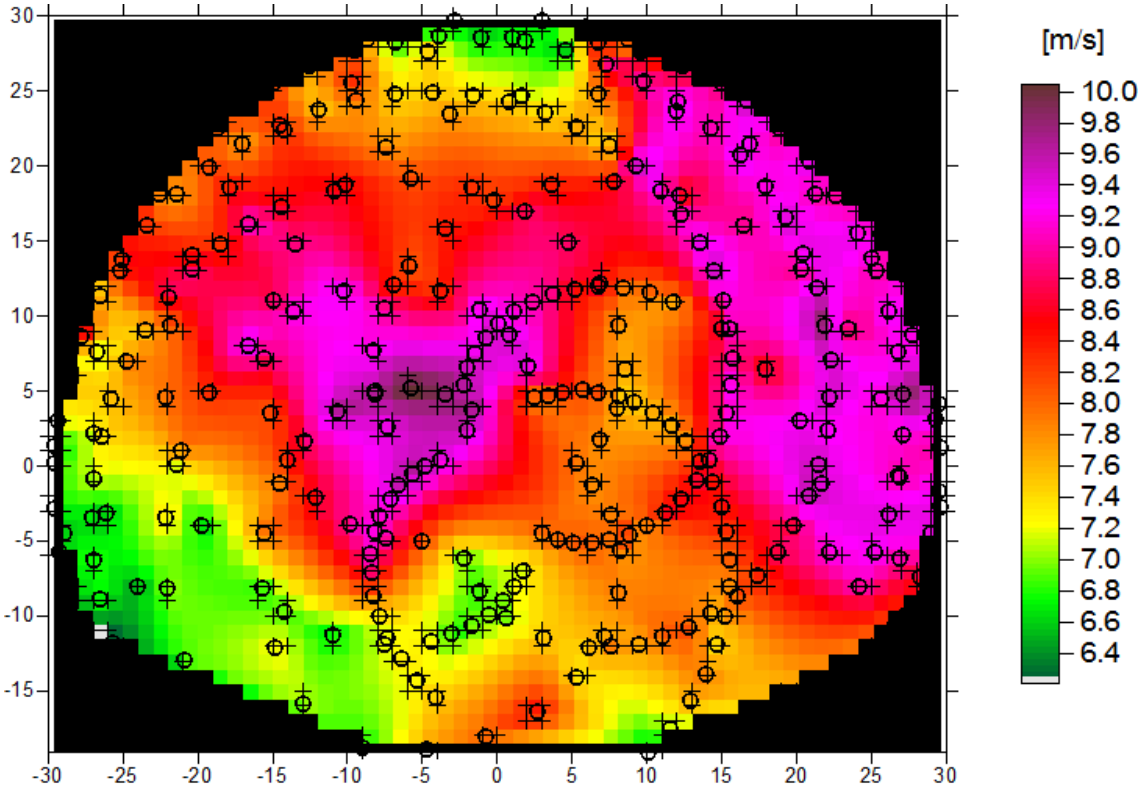

Figure 20. Calculated line of sight wind speeds for the real measurement points, interpolated to the grid. 61*51 calculation grid.

8. References

(): , Page , Publisher .

Astrup, P., Jensen, N.O., and Mikkelsen, T, (1996): Surface Roughness Model for LINCOM, Risø-R-900(EN), Risø National Laboratory, Denmark

Ib Troen, Ib and de Baas, Anne (1986): A spectral diagnostic model for wind flow simulation in complex terrain, Page 37-41, in Proceedings of the European Wind Energy Association Conference & Exhibition, Rome.

DTU Wind Energy is a department of the Technical University of Denmark with a unique integration of research, education, innovation and public/private sector consulting in the field of wind energy. Our activities develop new opportunities and technology for the global and Danish exploitation of wind energy. Research focuses on key technical-scientific fields, which are central for the development, innovation and use of wind energy and provides the basis for advanced education at the education.

We have more than 240 staff members of which approximately 60 are PhD students. Research is conducted within nine research programmes organized into three main topics: Wind energy systems, Wind turbine technology and Basics for wind energy.

Danmarks Tekniske Universitet
DTU Vindenergi
Nils Koppels Allé
Bygning 403
2800 Kgs. Lyngby
Telephone 45 25 25 25

info@vindenergi.dtu.dk
www.vindenergi.dtu.dk